Simultaneous topology and sizing optimization of viscous dampers in seismic retrofitting of 3D irregular frame structures

Oren Lavan and Oded Amir
Faculty of Civil and Environmental Engineering, Technion - Israel Institute of Technology

1 Abstract

A new methodology for performance-based optimal seismic retrofitting using a limited number of size groups of viscous dampers is presented. The damping coefficient of each size group of dampers is taken as a continuous variable and is determined by the optimization algorithm. Furthermore, for each potential location, a damper of a single size group is optimally assigned, if any. Hence, the formulation presents a large step forward towards practical optimal design of dampers. The key for achieving an efficient optimization scheme is the incorporation of material interpolation techniques which were successfully applied in other structural optimization problems of discrete nature. This results in a very effective optimization methodology, that is expected to be very efficient for large scale structures. The proposed approach is demonstrated on several example problems of 3D irregular frame structures.

Keywords : energy dissipation devices; viscous dampers; seismic retrofitting; irregular structures; asymmetric structures; topology optimization; material interpolation functions

2 Introduction

With the growing body of knowledge in the field of Earthquake Engineering, it is realized that many existing structures do not comply with life safety requirements of modern codes. Furthermore, nowadays performance based design (PBD - [10, 41]), where the performance of the structure after an earthquake also serves as a design criterion, seems to gain prominence, and damage is to be limited. Hence, it is sometimes desired to enhance the seismic performance of existing structures. An effective approach of enhancing the seismic performance of existing structures, while limiting their structural as well as nonstructural damage, makes use of energy dissipation devices (e.g. [45, 13, 50]). With the right design, these could appreciably reduce inter-story drifts in the structure. Furthermore, energy is dissipated by these devices rather than in the buildings. Thus the main damage criteria are directly targeted.

Out of the variety of energy dissipation devices, the efficiency of viscous dampers in reducing various seismic responses has been shown for both frame [14, 29] and wall [27] buildings. This statement holds, in particular, in the case of retrofitting due to the out-of-phase effect that may eliminate the need for foundation and columns strengthening [14, 27].

Design methods for the seismic retrofitting of frame structures using viscous dampers have been proposed in the literature (see e.g. [23], [39] and references therein). It has been shown, however, that the distribution of damping may appreciably affect its efficiency [21]. Therefore, design methods that lead to efficient distributions may have a crucial effect on the cost of retrofitting. Consequently, it may also determine whether viscous dampers will be preferred over other technologies. Thus, optimal design methods are of much importance. Consequently, considerable efforts were invested in developing optimal design methods for the seismic retrofitting of frame structures using viscous dampers (see e.g. [4, 5, 18, 38, 43, 49, 55, 53] and references therein). Most of the research was focused, however, on symmetric and regular structures. Thus, most approaches adopted a plane model of the building.

Experience shows that irregular structures are seismically more vulnerable than their regular counterparts. This is often due to the large deformations and ductility demands concentrated

at the region of irregularity. Furthermore, the seismic behavior of irregular structures is often harder to predict, by means of simplified analysis tools, than the behavior of regular ones. Thus, more advanced analysis tools are to be adopted. This often leads to more complex optimization problems. Nevertheless, a few works also tackled the optimal design problem of viscous damping in retrofitting of 3D irregular structures (e.g. [54, 19, 51, 20, 35, 26, 36, 37, 32, 33, 17, 3, 2]). In particular, Lavan and Levy [32] minimized the total added damping while constraining the envelope peak inter-story drift of each peripheral frame in each story separately. The envelope was taken from all ground motions in the ensemble considered while the peak was taken in time. As each inter-story drift was constrained separately, a concentration of added damping, only where needed, was resulted [34]. This prevented large local responses, as usually observed in irregular structures. Furthermore, constraining the inter-story drifts to allowable values enabled the use of the optimization methodology in a PBD framework.

Most of the abovementioned approaches adopt continuous design variables (damping coefficients of the dampers). As, in practice, damping coefficients are adapted for each project, the damping coefficient is indeed a continuous variable. Nonetheless, the development of each size group of dampers, and its prototype testing, dictate an additional cost for each size group of dampers used (i.e. for each group of dampers with similar properties). Hence, while the damping coefficient of each size group of dampers is a continuous variable, the number of size groups of dampers to be used in each project is usually limited. Indeed, the various continuous optimal damping coefficients attained could be rounded and grouped to only a few size groups. While practically, this is expected to lead to good designs in the majority of cases, this cannot be guaranteed in general. Furthermore, there is no straightforward manner to choose the damping coefficients of the various size groups.

Methodologies have also been proposed for the design and optimal design of dampers using discrete values for the damping coefficients ([56, 1, 38, 15, 29, 24]). Each of these approaches has its strengths and weaknesses in terms of: the problem formulation and the flexibility of the approach of adopting other formulations; the computational effort and its scalability in cases of large scale structures; the modeling approach used for the ground motion hazard and the building and assumptions made on its behavior, etc. Furthermore, all methods make use of predetermined parameters for the damping: either the dampers' sizes; the damping increment; the number of dampers; or a combination of those. The use of predetermined parameters, and the values adopted, may have a considerable effect on the optimal solution. While some engineering judgment may be used to attain good values for these parameters, it could be a huge step forward if those could be optimally set by the optimization scheme. Additionally, the schemes adopted in the literature for treating problems with discrete variables are, in principle, combinatorial optimization methods. Thus, the computational effort appreciably grows with the number of discrete design variables, limiting the discussion to small scale structures.

Structural optimization problems of a discrete nature often arise in the sub-discipline of topology optimization. Topology optimization is a computational method aimed at optimizing the distribution of one or several materials in a given continuum design domain. Following intense research since its introduction by Bendsøe and Kikuchi [7], the method is now considered an integral part of the design process of load-bearing structural components in the automotive and aircraft industries [42]. For a comprehensive survey of the method and its applications, the reader is referred to the monograph by Bendsøe and Sigmund [9]. Topology optimization techniques are strongly coupled to continuum finite element analysis, where the topological layout of the structure is represented by the existence of material in each finite element in the discretized model of the design domain. In principle, this leads to large-scale 0-1 integer optimization problems: The optimizer should determine whether to assign solid material (represented by a density value of 1) or void (density value of 0) in each finite element. From a mathematical standpoint, such problems are very difficult to solve due to the number of possible solutions which increases exponentially with the number of finite elements. Material interpolation functions are the key development that enables the solution of such 0-1 problems in large scale. Instead of binary variables they utilize *continuous* variables in the interval $[0, 1]$ while *penalizing* intermediate values. In the classical context of finding the stiffest structure for a given available volume, penalization means that intermediate densities (between 0 and 1) are assigned relatively low stiffness so that they become uneconomical. This drives the optimized design towards 0-1 solutions consisting of either solid material or void, but without actually solving an integer optimization problem. The problem to be solved herein is intended to consider optimal damper placement and sizing in large scale 3D structures. Hence,

the number of potential locations for the dampers, and the number of size groups of dampers to be considered, could lead to a large number of discrete design variables. In order to facilitate the efficient solution of such problems, material interpolation techniques, proven efficient in topology optimization, are adopted.

The optimization problem formulation in this paper adopts the same constraints presented by Lavan and Levy [32] so as to enable a PBD of 3D irregular structures under a realistic ensemble of ground motions. This paper, however, presents a first step of using topology optimization tools in optimal seismic design. This enables to consider more realistic and practical design variables and objective functions than those used in [32] or those used in the literature where discrete values for the damping coefficients were considered. In the formulation proposed herein, dampers of similar properties, which are taken as continuous variables and are determined by the optimization algorithm and not a-priori, are optimally allocated by the algorithm. That is, both the damper size group to be assigned at each potential location and the damping coefficient of each size group of dampers serve as design variables while the former are of a discrete nature and the latter are continuous. In addition, the number of dampers used in a given design is flexible while is properly accounted for in the cost function. Furthermore, the formulation of the optimization problem using continuous variables and interpolation functions, and the first order optimization tools adopted, lead to a computationally efficient algorithm. In the current study we solve design problems with either one or two damper sizes. Nevertheless, the formulation is general and further investigations with a wider selection of dampers will be pursued in the near future.

The remainder of the article is organized as follows: The earthquake engineering design problem is stated in Section 3. The mathematical formulation incorporating material interpolation functions is presented in Section 4, where specific details are given also regarding the implementation. Several demonstrative examples are given in Section 5, followed by a discussion in Section 6.

3 Problem definition

3.1 Equations of motion

When retrofitting a structure using viscous dampers, linear behavior of the damped structure is often desired. Using the proposed methodology, as will be elaborated later on, inter-story drifts could be constrained to allowable limits. Thus, those limits could be set to assure a linear behavior, if feasible. Furthermore, linear dampers are adopted due to their out-of-phase effect [14]. Once designed, those could be replaced with equivalent nonlinear ones if desired. One approach for that is by equating the dissipated energy per cycle in the two dampers (linear and nonlinear) with the peak displacement expected (see e.g. [48]). Hence, it is assumed here that the behavior of the damped structure could be assessed using the linear equations of motion. Furthermore, rigid diaphragms are assumed while only the two horizontal components as well as one rotational component of the ground motion (about a vertical axis) are considered. Thus, the equations of motion, for a 3D irregular structure, can be written as follows:

$$\mathbf{M}\ddot{\mathbf{u}}(t) + [\mathbf{C}_s + \mathbf{C}_d]\,\dot{\mathbf{u}}(t) + \mathbf{K}\mathbf{u}(t) = -\mathbf{M}\mathbf{e}\mathbf{a}_g(t), \qquad \dot{\mathbf{u}}(0) = \mathbf{u}(0) = \mathbf{0}$$

where $\mathbf{M}$, $\mathbf{C}_s$ and $\mathbf{K}$ are the mass, inherent damping and stiffness matrices of the structure, respectively; $\mathbf{C}_d$ is the added damping matrix whose entries are to be determined in the optimization process; $\mathbf{u}(t)$, $\dot{\mathbf{u}}(t)$ and $\ddot{\mathbf{u}}(t)$ are the displacements, velocities and accelerations at the degrees of freedom relatively to the ground as a function of time, t; $\mathbf{e}$ is the excitation direction matrix; and $\mathbf{a}_g(t)$ is a vector with the ground motion acceleration components as a function of time. Note that the structural properties are of a stochastic nature. Often, for the assembly of the matrices of the structure, their nominal values are adopted. For more details on the effect of their probability distribution on the actual response of the structure the reader is referred to [28].

The dampers' local coordinates are, in general, different from the global coordinates used. Thus, a transformation of coordinates is useful in assembling the added damping matrix (e.g. [12]). This transformation takes the form

$$\mathbf{C_d}(\mathbf{c}_d) = \mathbf{T}^T D(\mathbf{c}_d)\mathbf{T}$$

where the vector $\mathbf{c}_d$ contains the damping coefficients at all potential locations of added dampers; $\mathbf{T}$ is a transformation matrix from global coordinates to the local coordinates of the dampers (damper elongation); and D is an operator that transforms a vector into a diagonal matrix.

3.2 Objective function and design parametrization

The overall aim of this study is to suggest a realistic optimization approach for minimizing the cost of retrofitting. The cost of retrofitting is taken as the number of dampers of each size group times the cost of a single damper of that size group. In general, the cost of a fluid viscous damper is a function of the force it is designed to sustain, its stroke (maximum elongation) and its damping coefficient. The latter has a minor direct effect on the cost but it influences the cost indirectly through its effect on forces as elaborated in the following. In frame structures the peak strokes of dampers that are located between adjacent floors are strongly correlated to the inter-story drifts. In addition, in the formulation presented herein, inter-story drifts (thus, indirectly, dampers' strokes) are constrained to allowable values. Thus, these are already accounted for in the formulation. Furthermore, the allowable values for inter-story drifts used in practice usually lead to strokes of the dampers that are smaller than standard stroke capacities supplied by manufacturers. Hence, these will also not be taken into account as components of the cost. Thus, the cost of a damper is taken here to be proportional to the force it is designed to sustain.

Within a group of dampers of the same size group, all dampers are designed to have the same properties. Hence, each damper of a given size group, regardless of the peak force it is expected to experience, is designed to sustain the maximum of peak forces expected in all individual dampers of that size group. Thus, the peak force in the most loaded damper of a given size group is taken as the cost measure of any individual damper of that size group.

Assuming a dominant mode behavior, the inter-story velocity at location j is proportional to $\omega_1 d_j$. Here ω_1 is the dominant mode frequency and d_j is the envelope peak drift at the location j. Experience shows that a damper is usually assigned to a location where the drift reaches its allowable value. As this value is predetermined here, an estimate for the maximum velocity of all dampers is known in advance. Hence the damping coefficient of each size group of damper is proportional to the peak force in the most loaded damper of that size group. This will be adopted herein as the cost of a single damper of a given size group.

As mentioned earlier, the cost of retrofitting is taken as the number of dampers of each size group times the cost of a single damper of that size group. Thus, the cost of retrofitting can be estimated as proportional to

$$J = \sum_{n=1}^{N_{sizegroups}} N_n c_n \tag{1}$$

where $N_{sizegroups}$ is the number of size groups of dampers considered, N_n is the number of dampers of size group n and c_n is the damping coefficient associated with damper size group n (that is proportional to the peak force in the most loaded damper of that size group).

In practice, each damper should be carefully designed so as to attain a desired force-velocity behavior. Furthermore, modern seismic codes require that a prototype of each size group of damper will be tested so as to verify its force-velocity behavior (e.g. [16]). Consequently, the number of size groups of dampers to be used in a given building is usually small. Nonetheless, the damping coefficient for each size group of dampers is determined by the engineer for each project separately.

For that purpose, the damping coefficients c_n should be represented by continuous design variables in the optimization problem. At the same time, the existence of a certain damper at a certain potential location should be represented by a discrete design variable that can attain a value of either zero or one. Therefore the damping coefficient at a certain location, denoted $c_{d,j}$, can be represented by the following statement

$$\begin{aligned} c_{d,j} &= \sum_{n=1}^{N_{sizegroups}} x_{jn} c_n \\ x_{jn} &\in \{0,1\} \\ \sum_{n=1}^{N_{sizegroups}} x_{jn} &\in \{0,1\} \qquad j = 1, ..., N_d \end{aligned}$$

where the double-indexed binary variable x_{jn} represents the existence of a damper of size group n in location j. Note that a binary constraint is imposed to ensure that only one damper size group can occupy a certain location. Alternatively, this requirement can be incorporated into the expression for the actual damping coefficient, following common topology optimization and

material interpolation approaches as discussed more thoroughly in Section 4. For example, in case there are two possible size groups of dampers one can rewrite

$$\mathbf{c}_d = D\left(\mathbf{x}_1\right)\left[c_1\mathbf{1} + \left(c_2 - c_1\right)\mathbf{x}_2\right]. \tag{2}$$

Note that the binary variables $\mathbf{x}$ are now organized in two vectors where the j-th entry in $\mathbf{x}_1$ determines the existence of a damper at a certain location j, while the j-th entry in $\mathbf{x}_2$ determines which size group will be assigned at that location - c_1 or c_2. Using this approach several size groups of dampers could be potentially considered. For each additional size group of damper considered, an additional continuous design variable is added - its damping coefficient. Furthermore, an additional binary design variable is added for each potential location. For a large number of damper size groups such a function may be a bit cumbersome to write. On the other hand, by utilizing (2) we avoid imposing a constraint on every location j - an advantage in case the optimization algorithm is not specifically tailored to treat a large number of sparse linear constraints. In the current study we experiment with up to two size groups of dampers and adopt the function (2). As the number of size groups of dampers to be used in a project is relatively small, this approach leads to a relatively small number of continuous design variables of type c_n. At the same time, for large scale structures, the number of potential locations dictating the size of the binary design vectors $\mathbf{x}_1$ and $\mathbf{x}_2$ may be large. This justifies the adoption and modification of efficient methods for large scale problems as suggested in this study.

In frame structures dampers are usually located within the stories. In 3D structures, so as to fully take advantage of the dampers for torsion control, they would usually be allocated on the peripheral frames. Thus, although the methodology to be proposed is not limited to certain locations for the dampers, their potential locations will usually be taken within each story of each peripheral frame.

3.3 Responses of interest - constraints

Damage due to earthquakes is generally divided into structural and nonstructural. The main responses that indicate structural damage are inter-story drifts; ductility demands in the plastic hinges forming in structural elements; and hysteretic energy dissipated in these plastic hinges. In frame structures ductility demands are strongly associated to the peak inter-story drifts. Moreover, the contribution of hysteretic energy to common damage measures is relatively small for most earthquakes (e.g. [40]). Thus, inter-story drifts may serve as an appropriate measure for structural damage. Furthermore, when using energy dissipation devices, a linear behavior of the damped structure is often desired and structural damage may be negligible. In such cases, nonstructural damage becomes dominant. Inter-story drifts are also the main responses that indicate on nonstructural damage for many types of nonstructural components (e.g. infill walls, piping etc.) Thus, in this work inter-story drifts are adopted as the responses of interest.

In irregular structures the distribution of inter-story drifts along the height of the structure, as well as in plan, is far from being uniform. Often, large inter-story drifts are observed in the vicinity of irregularity and excessive local damage may be resulted. In order to comply with the PBD framework, peak inter-story drifts at selected locations are constrained to allowable values, *for each location separately*. This also enables constraining the response so as to result in a linear behavior. These are actually peak values of linear combinations of the displacements of the degrees of freedom. Mathematically, they can be formulated as follows:

$$\mathbf{d}_c = \max_t \left(\left| [D(\mathbf{d}_{all})]^{-1} \mathbf{H}\mathbf{u}(t) \right| \right)$$

where $\mathbf{d}_c$ is the vector of displacements (inter-story drifts) to be controlled; $\max_t(\cdot)$ is the maximum of the expression in the parentheses over time; $|\cdot|$ denotes the absolute operator; $\mathbf{d}_{all}$ is a vector of allowable values for $\mathbf{d}_c$; and $\mathbf{H}$ is a transformation matrix from global coordinates to the coordinates of $\mathbf{d}_c$ (those to be constrained). Note that as the displacements to be controlled are normalized by $\mathbf{d}_{all}$ a value of one indicates a displacement that equals its allowable value. Hence, these should be constrained to unity.

It should be emphasized that constraining performance measures to allowable values fits well within the PBD philosophy. Here, the engineer could determine the limits allowed for inter-story drifts while minimizing the cost and not vice-versa. Furthermore, the limits could be set so as to assure a linear behavior as assumed. However, if for some reason it is desired to minimize the response while constraining the cost, the methodology hereby presented could accommodate that.

3.4 Optimization problem

The optimization problem to follow is formulated based on the preceding sections. We focus on design with up to two damper size groups, even though the methodology can accommodate any number of damper size groups and potential damper locations. Continuous design variables are adopted for the damping coefficients of the various size groups of dampers. In principle, discrete variables should be adopted to indicate the size group of damper to be used at each potential location, if at all. The objective function considered mimics the maximum envelope peak force in the damper of any given size group as it is multiplied by the number of dampers of that size group. Constraints are added on the envelope peak inter-story drifts of the peripheral frames, at each story separately while side constraints on damping coefficients are also considered. Formally, this optimization problem can be stated as follows:

$$
\begin{aligned}
\min_{\mathbf{x}_1,\mathbf{x}_2,\mathbf{c}} J \quad &= \quad {\mathbf{x_1}}^T \left[c_1 \mathbf{1} + (c_2 - c_1)\, \mathbf{x}_2\right] \\
\text{s.t.:} \quad & \quad \mathbf{d}_c = \max_t \left(\left| [D(\mathbf{d}_{all})]^{-1} \mathbf{H}\mathbf{u}(t) \right| \right) \leq \mathbf{1} \qquad \forall \mathbf{a}_g(t) \in \mathcal{E} \\
& \quad x_{1,j} \in \{0,1\} \qquad j = 1, ..., N_d \\
& \quad x_{2,j} \in \{0,1\} \qquad j = 1, ..., N_d \\
& \quad \mathbf{0} \leq \mathbf{c} \leq \mathbf{c}_{max} \\
\text{with:} \quad & \quad \mathbf{M}\ddot{\mathbf{u}}(t) + \left[\mathbf{C}_s + \mathbf{C}_d\left(\mathbf{c}_d\left(\mathbf{x}_1, \mathbf{x}_2, \mathbf{c}\right)\right)\right] \dot{\mathbf{u}}(t) + \mathbf{K}\mathbf{u}(t) = -\mathbf{M}\mathbf{e}\mathbf{a}_g(t) \qquad \forall \mathbf{a}_g(t) \in \mathcal{E} \\
& \quad \dot{\mathbf{u}}(0) = \mathbf{0} \\
& \quad \mathbf{u}(0) = \mathbf{0}
\end{aligned} \tag{3}
$$

where $\mathcal{E}$ is the ensemble of ground motions considered; and $\mathbf{c}_{max}$ is a physical upper bound on the desired damping coefficients.

4 Optimization approach

The earthquake engineering design problem outlined above (3) involves both discrete and continuous design parameters. Thus in principle it could be tackled by mixed-integer programming methods, such as those applied by Kanno [24] for damper placement optimization with objectives based on transfer functions. However, due to the combinatorial nature of the optimization problem, the computational cost of integer programming algorithms tends to increase significantly with the number of design variables. This poses a certain limit on the number of damper locations and damper size groups that can be considered. In the current study, we propose an approach that utilizes only continuous variables but can result in practically discrete solutions. The key point is the application of well-established material interpolation techniques which have been developed over the past 25 years in the field of structural topology optimization.

4.1 Material interpolation techniques

Various material interpolation functions have been proposed in the context of topology optimization procedures. Up to date, the most commonly used is the SIMP model - Solid Isotropic Material with Penalization [6]. For the classical topology optimization task of distributing a given amount of material so that the stiffest structure is obtained, the SIMP model suggests a nonlinear relation between the material density ρ and Young's modulus

$$E(\rho) = \rho^p E^0$$

where $p \geq 1$ is the penalization power and E^0 is the reference stiffness for solid material ($\rho = 1$). For an extensive discussion of SIMP and several other interpolations, as well as their physical interpretation in continuum mechanics, the reader is referred to [8]. In the current study, we experimented with utilizing either SIMP or the so-called RAMP (Rational Approximation of Material Properties) interpolation function [47]. In our numerical experiments, the latter appeared more appropriate and provided promising results. Therefore the presentation from this point on is dedicated to the utilization of RAMP. For a certain density $0 \leq \rho \leq 1$, Young's modulus $E(\rho)$ is given by the RAMP interpolation as

$$E(\rho) = E_{min} + \frac{\rho}{1 + p(1-\rho)}(E_{max} - E_{min})$$

where E_{min} and E_{max} are the actual physical values corresponding to $\rho = 0$ and $\rho = 1$ respectively, thus accommodating both solid-void as well as two-material distributions. The SIMP and RAMP functions are sketched in Figure 1 for various values of p. For $p = 1$, $E(\rho)$ is a linear function, meaning that stiffness is directly proportional to the value of the density. Increasing p introduces a penalization effect so that intermediate values of the density design variable correspond to relatively weak material properties, implicitly leading to a preference of 0-1 designs.

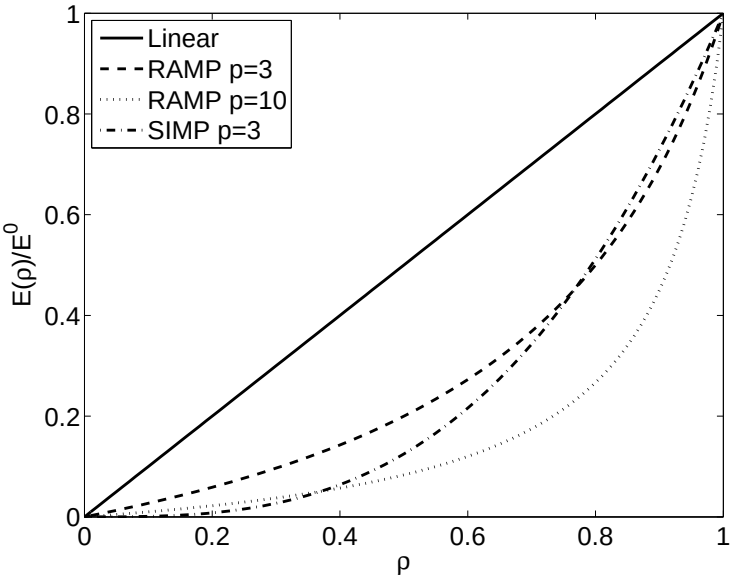

Figure 1: Examples of SIMP and RAMP material interpolation functions for various values of the penalty parameter p.

The concept of material interpolation and penalization of intermediate values in order to attain discrete solutions was successfully applied also in optimization of composite laminate structures. This was initially achieved using the DMO (Discrete Material Optimization) approach [46], and later extended to unified topology and multi-material optimization [22]. To the best of the authors' knowledge, the current contribution represents the first attempt to apply material interpolation techniques in structural optimization of seismic response. As reflected in the problem stated in Section 3, the basic design task involves finding optimal damper locations thus requires a formulation using discrete variables. In the following sections, we will reformulate the optimization problem using only continuous variables and apply penalization concepts to drive the optimized design towards discrete solutions.

4.2 Problem formulation and sensitivity analysis

In the following reformulation of (3), the cost of damping follows Eq. (2) and is given by

$$J(\mathbf{x}, \mathbf{y}) = \bar{c_d} \mathbf{x}_1^T \left[y_1 \mathbf{1} + (y_2 - y_1)\, \mathbf{x}_2 \right] \tag{4}$$

where $\bar{c_d}$ is a scaling parameter representing the maximum desired damping coefficient, and the actual damping coefficient of the two size groups of dampers is determined by y_1 and y_2. This enables all design variables $\mathbf{x}_1$, $\mathbf{x}_2$ and $\mathbf{y}$ to lie in the interval $[0, 1]$ thus avoiding ill-conditioning of the optimization problem. The $\mathbf{y}$ variables can have stricter limits if the user wishes to separate the feasible ranges of damping. Again, the existence of a damper in a specific location j is governed by the variable $x_{1,j}$. The damping coefficient is determined by the value of the variable $x_{2,j}$ that specifies the quantity between the limits of $\bar{c_d} y_1$ and $\bar{c_d} y_2$. Assuming a discrete (0-1) solution of the variables $x_{1,j}$ and $x_{2,j}$ can be obtained, it will correspond to having in location j one of three possibilities: 1) No damping; 2) A damping coefficient of $\bar{c_d} y_1$; or 3) A damping coefficient of $\bar{c_d} y_2$. One of the advantages of this approach is that the $\mathbf{y}$ variables are truly continuous thus the amount of damping is not specified a-priori.

Preference of 0-1 designs is achieved by assigning a *physical* damping coefficient which is different from the above cost (4) for the same set of values $\{\mathbf{x}_1, \mathbf{x}_2, \mathbf{y}\}$. This is achieved by relating

the physical damping coefficients $\widetilde{\mathbf{c}}_d$ to the design variables via nonlinear material interpolation functions, where intermediate values represent artificially low damping compared to the cost. For optimizing with two size groups of dampers, the effective damping in each potential location j is determined by a multiplication of two RAMP functions

$$\widetilde{c}_{d,j} = \bar{c_d} \frac{x_{1,j}}{1+p(1-x_{1,j})} \left(y_1 + (y_2 - y_1) \frac{x_{2,j}}{1+p(1-x_{2,j})} \right) \tag{5}$$

This leads to the following optimization problem statement

$$\begin{aligned}
\min_{\mathbf{x}_1,\mathbf{x}_2,\mathbf{y}} J(\mathbf{x},\mathbf{y}) \quad &= \quad \bar{c_d} \mathbf{x}_1^T \left[y_1 \mathbf{1} + (y_2 - y_1)\, \mathbf{x}_2 \right] \\
\text{s.t.:} \quad & \widetilde{d}_c = \frac{\mathbf{1}^T [D(\widetilde{\mathbf{d}}_c(t_f))]^{\frac{q+1}{r}} \mathbf{1}}{\mathbf{1}^T [D(\widetilde{\mathbf{d}}_c(t_f))]^{\frac{q}{r}} \mathbf{1}} \leq 1 \qquad \forall \mathbf{a}_g(t) \in \mathcal{E} \\
& 0 \leq x_k \leq 1 \qquad k = 1, 2, ..., 2j-1, 2j \\
& 0 \leq y_1^L \leq y_1 \leq y_1^U \leq 1 \\
& 0 \leq y_2^L \leq y_2 \leq y_2^U \leq 1 \\
\text{with:} \quad & \mathbf{M}\ddot{\mathbf{u}}(t) + \left[\mathbf{C}_s + \mathbf{C}_d \left(\widetilde{\mathbf{c}}_d \left(\mathbf{x}, \mathbf{y} \right) \right) \right] \dot{\mathbf{u}}(t) + \mathbf{K}\mathbf{u}(t) = -\mathbf{M}\mathbf{e}\mathbf{a}_g(t) \qquad \forall \mathbf{a}_g(t) \in \mathcal{E} \\
& \dot{\mathbf{u}}(0) = \mathbf{0} \\
& \mathbf{u}(0) = \mathbf{0} \\
& \widetilde{\mathbf{d}}_c = \left(\frac{1}{t_f} \int_{t_0}^{t_f} \left(\left[D\left(\mathbf{d}_{all} \right) \right]^{-1} D\left(\mathbf{H}\mathbf{u}\left(t \right) \right) \right)^r dt \right)^{\frac{1}{r}} \cdot \mathbf{1}
\end{aligned} \tag{6}$$

where $\widetilde{d}_c$ represents the aggregation of all constraints on inter-story drifts into a single differentiable constraint on the maximum component [32]; q is a large positive number; r is a large positive even number; y_1^L, y_1^U, y_2^L and y_2^U are user-defined bounds; and t_0 and t_f are the initial and final times. When multiplying the $\mathbf{y}$ variables by the scaling parameter $\bar{c_d}$, practical damping coefficients should be obtained. For optimizing the distribution and size of a single damper size group, only the $\mathbf{x}_1$ and y_1 variables are necessary, thus it can be seen as a particular case of the two-damper optimization.

Details regarding the numerical solution of the optimization problem will be given in the next section. We apply a Sequential Linear Programming (SLP) approach, in particular the cutting plane method [11, 25] with some modifications [30, 31, 32], as will be elaborated subsequently. For formulating the optimization sub-problem within each optimization cycle, first-order derivatives of the objective and of the general constraint are required. For the objective of (6) these are straightforward. For the general constraint in (6) an adjoint sensitivity analysis procedure was developed by Lavan and Levy [30]. Based on the adjoint procedure one can compute the sensitivity of the aggregated constraint on the drift with respect to the physical damping coefficient at a certain location j , i.e. $\frac{\partial \widetilde{d}_c}{\partial \widetilde{c}_{d,j}}$. Then, the actual sensitivities are computed by the chain rule

$$\begin{aligned}
\frac{\partial \widetilde{d}_c}{\partial x_{1,j}} \quad &= \quad \frac{\partial \widetilde{d}_c}{\partial \widetilde{c}_{d,j}} \frac{\partial \widetilde{c}_{d,j}}{\partial x_{1,j}} = \\
& \frac{\partial \widetilde{d}_c}{\partial \widetilde{c}_{d,j}} \bar{c_d} \left(\frac{1}{1+p(1-x_{1,j})} + \frac{p x_{1,j}}{(1+p(1-x_{1,j}))^2} \right) \left(y_1 + (y_2 - y_1) \frac{x_{2,j}}{1+p(1-x_{2,j})} \right) \\
\frac{\partial \widetilde{d}_c}{\partial x_{2,j}} \quad &= \quad \frac{\partial \widetilde{d}_c}{\partial \widetilde{c}_{d,j}} \frac{\partial \widetilde{c}_{d,j}}{\partial x_{2,j}} = \\
& \frac{\partial \widetilde{d}}{\partial \widetilde{c}_{d,j}} \bar{c_d} \frac{x_{1,j}}{1+p(1-x_{1,j})} (y_2 - y_1) \left(\frac{1}{1+p(1-x_{2,j})} + \frac{p x_{2,j}}{(1+p(1-x_{2,j}))^2} \right) \\
\frac{\partial \widetilde{d}_c}{\partial y_1} \quad &= \quad \sum_{j=1}^{N_d} \frac{\partial \widetilde{d}_c}{\partial \widetilde{c}_{d,j}} \frac{\partial \widetilde{c}_{d,j}}{\partial y_1} = \sum_{j=1}^{N_d} \frac{\partial \widetilde{d}}{\partial \widetilde{c}_{d,j}} \bar{c_d} \frac{x_{1,j}}{1+p(1-x_{1,j})} \frac{1-x_{2,j}}{1+p(1-x_{2,j})} \\
\frac{\partial \widetilde{d}_c}{\partial y_2} \quad &= \quad \sum_{j=1}^{N_d} \frac{\partial \widetilde{d}_c}{\partial \widetilde{c}_{d,j}} \frac{\partial \widetilde{c}_{d,j}}{\partial y_2} = \sum_{j=1}^{N_d} \frac{\partial \widetilde{d}}{\partial \widetilde{c}_{d,j}} \bar{c_d} \frac{x_{1,j}}{1+p(1-x_{1,j})} \frac{x_{2,j}}{1+p(1-x_{2,j})}
\end{aligned}$$

4.3 Computational implementation

Successful utilization of existing computational methods for solving the nonlinear, non-convex optimization problem at hand requires several practical measures. These will be discussed in this section with the aim of providing a clear and transparent description of our implementation. In particular, we discuss: 1) The treatment of an ensemble of ground motions; 2) Adding and removing constraints; and 3) Continuation schemes for parameter control.

Considering an ensemble of ground motions In principle, the complete ensemble of ground motions should be considered within every design cycle when solving (6). However, this is not an efficient approach and is by no means necessary. In the current study, we repeat the procedure suggested by Lavan and Levy [30] where the first "active" ground motion is chosen according to the spectral displacements corresponding to the structure's natural period. Following the optimization with this single ground motion, additional ground motions are considered in case the constraint is violated. Optimization and feasibility checks are repeated until no violation is encountered with the optimized design.

Adding and removing constraints As mentioned above, we apply a modified version of the cutting plane method for solving (6). This follows the successful utilization of the method in previous studies on optimization of added damping based on continuous design variables (e.g. [30, 31, 32]). Within each optimization cycle, a linear sub-problem is generated and solved. In the standard cutting plane method, the linear sub-problem expands within every design cycle when a new linear constraint is added. For non-convex problems some of the linearized constraints might be conservative with respect to the original problem, meaning they may be active even though the solution is located well within the actual (nonlinear, non-convex) feasible region. Such linearized constraints are nullified and disregarded in subsequent design cycles, as proposed by Lavan and Levy [30].

Continuation schemes for parameter control The optimization problem (6) includes several highly nonlinear components - namely the penalized effective damping coefficient (5) and the differential equivalents of the maximum and absolute value operators in the aggregated constraint. Therefore difficulties in finding a good optimized solution are expected. A common approach for avoiding divergence of the optimization process is to gradually increase the parameters that control the degree of nonlinearity. This applies to the penalization power p as well as the parameters r and q in (6). Furthermore, a conservative move limit is imposed in the solution of the linear sub-problems, meaning that updates of $\mathbf{x}_1$, $\mathbf{x}_2$ and $\mathbf{y}$ are restricted to a close neighborhood of the solution corresponding to the previous sub-problem. Specific details regarding the values of these parameters are given in the descriptions of the solved examples.

5 Examples

In this section we present several examples, demonstrating the effectiveness of the optimization approach proposed in this article. In all examples we use the LA 10% in 50 years ensemble of ground motions (see [44] for details). Furthermore, we assume 5% of critical damping for the first two modes in order to construct the Rayleigh damping matrix of the structures. The optimization process was stopped once all three requirements were satisfied: 1) The maximum change in the value of a design variable was smaller than 1E-3; 2) The absolute value of the constraint on the actual normalized drifts was smaller than 1E-3; and 3) The penalty value p reached its target value. For numerical experiments a single-processor MATLAB code was executed on a standard PC with a 2.4GHz CPU.

5.1 Example 1: Two-story plane shear frame

The first example examines the optimal added damping for a two-story shear frame presented by Levy and Lavan [33], see Figure 2. There, optimal design of added dampers was attained using uncorrelated continuous design variables for the damping coefficients of the dampers in the first and second stories. As there are only two potential locations for dampers, contours of the constraint and objective function can be visualized in the damping coefficients' plane.

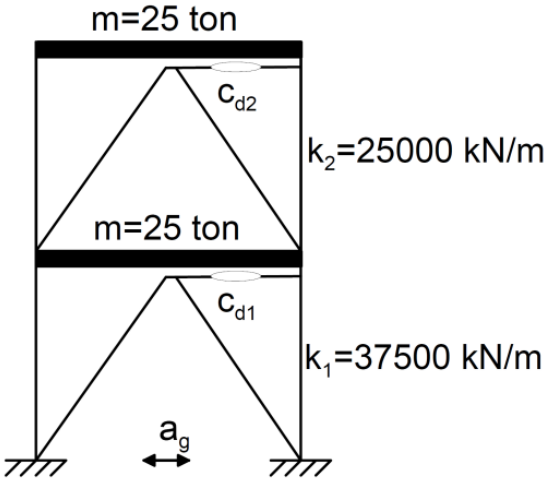

Figure 2: A two story plane shear frame for example 1.

For the sake of completeness, the mass, inherent damping and stiffness matrices are given below. Also given are the excitation direction vector and transformation matrix from global coordinates to local coordinates of the dampers.

$$\mathbf{M} = \begin{pmatrix} 25 & 0 \\ 0 & 25 \end{pmatrix} ton \; ; \; \mathbf{C}_s = \begin{pmatrix} 120.7 & -32.4 \\ -32.4 & 72.1 \end{pmatrix} \frac{kN \cdot s}{m} \; ; \; \mathbf{K} = \begin{pmatrix} 62500 & -25000 \\ -25000 & 25000 \end{pmatrix} \frac{kN}{m}$$

$$\mathbf{e} = \begin{pmatrix} 1 \\ 1 \end{pmatrix} \; ; \; \mathbf{T} = \begin{pmatrix} 1 & 0 \\ -1 & 1 \end{pmatrix}$$

As in [33], a single ground motion LA02 was considered for design. The allowable inter-story drift was set to $0.009m$. In the solutions reported by Levy and Lavan [33] a total added damping of $1,482 \left[\frac{kN \cdot s}{m}\right]$ and $1,454 \left[\frac{kN \cdot s}{m}\right]$ using a "fully stressed design" criterion and gradient-based optimization respectively. Note that the convergence criteria were different using these two approaches hence the differences. Here, we apply the proposed formulation to demonstrate the capability of achieving a binary design with a single size group of damper.

The optimization problem (6) was solved with the following parameters: Maximum nominal damping $\bar{c_d} = 3000 \left[\frac{kN \cdot s}{m}\right]$; initial solution $x_1 = [0.5, 0.5]$, $y_1 = 1$; iterative move limit $= 0.1$; initial penalty $p = 1$, multiplied by 1.5 every 10 design iterations, up to $p = 100$; initial $r = 1000$, raised by 50 every design iteration; and initial $q = 1000$, raised by 50 every design iteration. The process converged after 121 iterations and the optimized damping was $1,104.2 \left[\frac{kN \cdot s}{m}\right]$ in each of the dampers while dampers were assigned to both the first and second stories (a total of $2,208.4 \left[\frac{kN \cdot s}{m}\right]$). The actual constraint violation was only 0.06% at the bottom floor, meaning a practically viable design was achieved. Looking at the contours of the objective and constraint plotted in Figure 3, it is clear that the proposed procedure succeeded in finding the globally optimal binary design, despite formulating the problem with continuous variables only.

5.2 Example 2: Eight-story three bay by three bay asymmetric structure

One of the evident advantages of the proposed approach is the capability to find optimized discrete designs with a large number of potential damper locations, in short computing time. In this example we consider a classical test case of an asymmetric reinforced concrete frame introduced by Tso and Yao [52]. A plan and two elevations of this structure are given in Figure 4. The column sizes are $0.5m \times 0.5m$ in frames 1 and 2; and $0.7m \times 0.7m$ in frames 3 and 4. The beam sizes are $0.4m \times 0.6m$ and the floor mass is uniformly distributed with a magnitude of $0.75 \frac{ton}{m^2}$. Optimal design of added dampers was attained by [32] using uncorrelated continuous design variables for the damping coefficients. As in [32] the design is to be attained for a single component of the ground motion in the "Y" direction using the whole ensemble. Note, however, that both the methodology

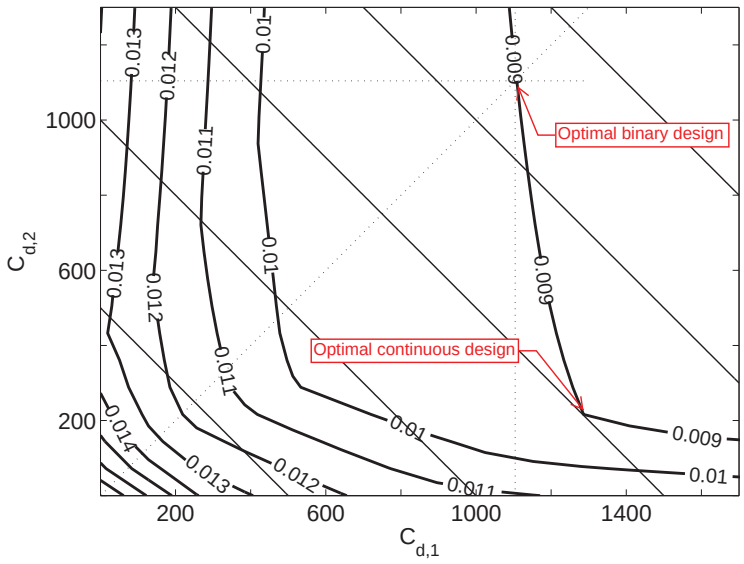

Figure 3: Graphical representation of the two-story frame optimization. Contours of the drift constraint appear in solid thick lines and contours of the objective in solid thin lines. Optima for both continuous and binary designs are marked. The computational procedure achieves the exact optimum for a discrete design, namely $c_{d,1} = c_{d,2} = 1104.2 \left[\frac{kN \cdot s}{m}\right]$.

presented by Lavan and Levy [32] and the methodology developed here are capable of considering all components of the ground motion.

Based on the discussion by [32], only 16 potential locations for the dampers were assigned, as presented in Figure 4. The allowable inter-story drift was set to $0.035m$ and the initial ground motion considered was LA16. First, a binary design with a single size group of damper was pursued, with the following parameters: Maximum nominal damping $\bar{c}_d = 50000 \left[\frac{kN \cdot s}{m}\right]$; initial solution $\mathbf{x}_1 = \mathbf{1}$, $y_1 = 1$; iterative move limit = 0.1; initial penalty $p = 1$, multiplied by 1.25 every 10 design iterations, up to $p = 100$; initial $r = 100$, raised by 50 every design iteration; and initial $q = 100$, raised by 50 every design iteration. Clearly, the continuation scheme imposed on the parameters p, r, and q reflects a higher degree of conservativeness compared to the previous example, which is necessary due to the larger number of design variables and local minima solutions.

The process converged after 215 iterations, taking 41.5 seconds in MATLAB. A value of $y_1 = 0.4979$ was obtained, corresponding to an optimized damping coefficient of $24,895 \left[\frac{kN \cdot s}{m}\right]$. The chosen locations of the dampers are presented in Table 1. As can be seen, the solution of $\mathbf{x}_1$ (column 2 in Table 1) reflects an almost binary 0-1 design, which can be easily interpreted into a practical design. The selected damper configuration is presented in column 5. With the interpreted design, the maximum violation of the constraint was 0.9% at location 10, corresponding to the second story in frame 4. Finally, the optimized design was evaluated with the other 19 ground motions in the ensemble and no further constraint violations were encountered.

In Table 1 we provide also some information for comparing the current procedure to previous approaches that achieved strictly continuous designs (e.g. [32]). As expected, the total added damping in the binary design is higher. However, it should be more economical because it utilizes only a single damper size group. Evidently, performing a continuous-variable optimization and then "rounding" the result to attain a binary design will lead to inferior performance compared to the proposed approach which is based on material interpolation techniques. For example, it is not clear how one can choose a single damping coefficient based on the results in column 6, without diverging significantly from the optimum. Furthermore, in the current result no damper is placed in location 13, as opposed to the optimized design in the continuous approach. This emphasizes the potential of the interpolation-penalization approach as an effective computational tool for achieving economical added damping configurations. Due to the utilization of continuous variables, this approach is expected to be more efficient than mixed-integer methods. This point still needs to be thoroughly examined based on a detailed comparison - a goal to be pursued in future work.

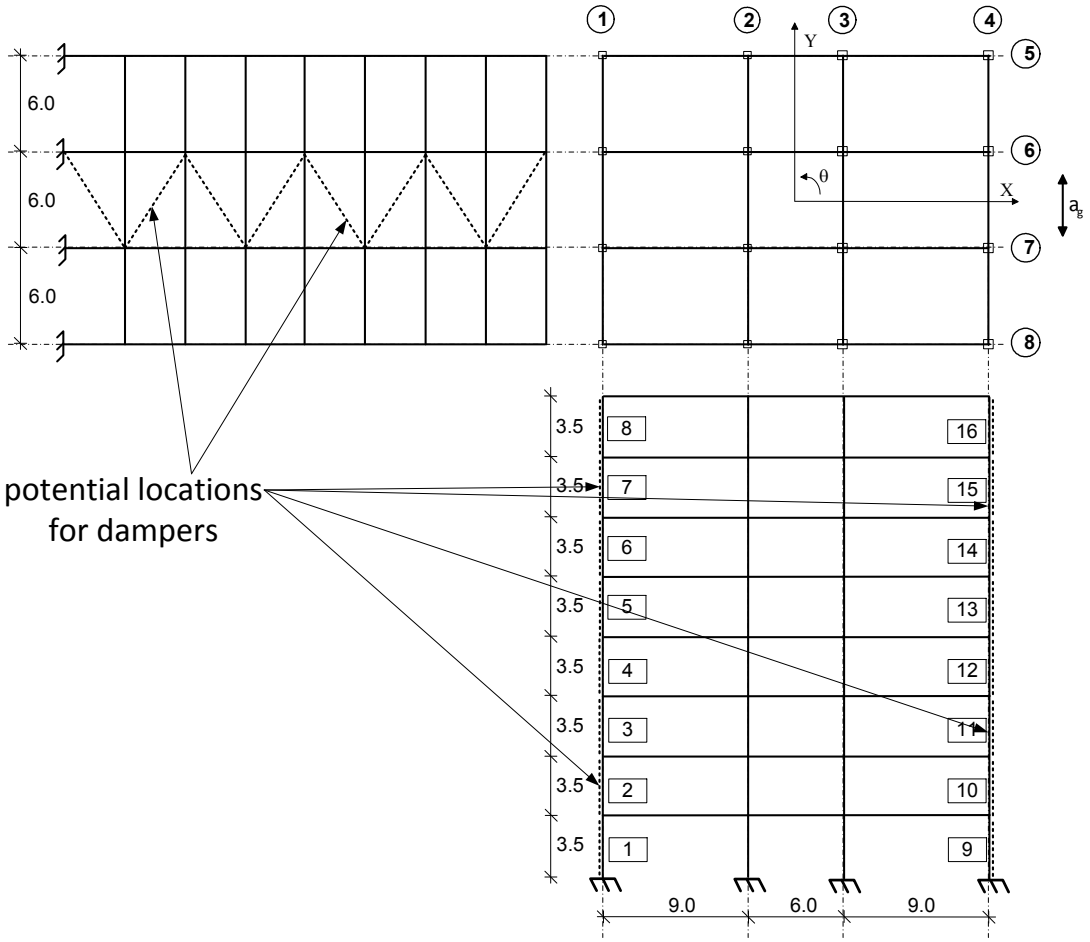

Figure 4: An asymmetric 3D frame structure for example 2 [52].

The same example is hereby utilized to demonstrate the capability of achieving optimized designs with several damper size groups whose coefficients are not defined a-priori. Optimization is now performed with two sets of variables $\mathbf{x}_1$ and $\mathbf{x}_2$ that are gradually "pushed" to attain binary values. Two size groups of dampers are available, with coefficients to be determined according to the values of the variables y_1 and y_2. The initial solution is: $\{\mathbf{x}_1 = 0.9 \cdot \mathbf{1}, \mathbf{x}_2 = 0.9 \cdot \mathbf{1}, y_1 = 0.45, y_2 = 0.9\}$. The bounds on y_1 and y_2 define a separate range for each of the two variables: $\left\{y_1^L = 0, y_1^U = 0.5, y_2^L = 0.5, y_2^U = 1\right\}$. The continuation scheme is slightly more conservative than for the single damper optimization: The penalty parameter is multiplied by 1.1 every 5 design iterations, up to $p = 150$. All other parameters remain unchanged.

The process converged after 268 iterations, taking 71.9 seconds in MATLAB. Values of $y_1 = 0.3923$ and $y_2 = 0.5468$ were obtained, corresponding to optimized damping coefficients of $19,615 \left[\frac{kN \cdot s}{m}\right]$ and $27,339 \left[\frac{kN \cdot s}{m}\right]$ respectively. The chosen locations of the dampers are presented in Table 2. In the solution of $\mathbf{x}_1$ and $\mathbf{x}_2$ in columns 2-3 there are a few entries that did not reach binary 0-1 values. In particular, we find it important to discuss the physical meaning of values such as $x_{3,2} = 0.3076$ and $x_{12,2} = 0.0330$. From a strictly mathematical standpoint, these are clearly not binary solutions as one would like to obtain. Nevertheless, from a physical perspective they are almost binary because their actual damping coefficient is very close to the damping corresponding to $x_{j,2} = 0$ - this is the result of high penalization. Therefore interpretation into a practical design as presented in column 6 is straightforward: The actual influence of reducing the damping coefficient from $19,637$ and $19,616$ to $19,615$ is very small. In the case of non-binary results such as $x_{5,1} = 0.9978$ and $x_{11,1} = 0.9995$ the implications are even less significant, because the cost is already very close to the cost for $x_{j,1} = 1$ and only the physical damping is relatively low due to penalization. This means that by setting $x_{5,1} = 1$ and $x_{11,1} = 1$ in the interpretation phase we just add physical damping practically for free. With the interpreted design, the maximum violation of

Location	$\mathbf{x}_1$	$\mathbf{c}_d$	$\widetilde{\mathbf{c}}_d$	Selected damper	Continuous design
1	1.0000	24,895	24,895	24,895	1,758
2	0.9998	24,890	24,441	24,895	32,472
3	1.0000	24,895	24,895	24,895	23,364
4	0.9963	24,803	18,117	24,895	19,241
5	0.9857	24,538	10,092	24,895	12,954
6-9	≈ 0	≈ 0	≈ 0	none	≈ 0
10	1.0000	24,895	24,895	24,895	24,183
11	1.0000	24,895	24,895	24,895	28,984
12	1.0000	24,895	24,895	24,895	16,743
13	≈ 0	≈ 0	≈ 0	none	2,005
14-16	≈ 0	≈ 0	≈ 0	none	≈ 0
				$\sum = 199,160$	$\sum = 161,700$

Table 1: Single damper optimization of the eight-story asymmetric structure. All damping coefficients are in $\left[\frac{kN \cdot s}{m}\right]$.

the constraint was 0.2% at location 2, corresponding to the second story in frame 1. Finally, the optimized design was evaluated with the other 19 ground motions in the ensemble and no other constraint violations were encountered.

Location	$\mathbf{x}_1$	$\mathbf{x}_2$	$\mathbf{c}_d$	$\widetilde{\mathbf{c}}_d$	Selected damper
1	1.0000	≈ 0	19,615	19,615	19,615
2	1.0000	1.0000	27,339	27,339	27,339
3	1.0000	0.3076	21,991	19,637	19,615
4	1.0000	≈ 0	19,615	19,615	19,615
5	0.9978	1.0000	27,280	20,540	27,339
6	≈ 0	≈ 0	≈ 0	≈ 0	none
7	≈ 0	≈ 0	≈ 0	≈ 0	none
8	≈ 0	≈ 0	≈ 0	≈ 0	none
9	≈ 0	1.0000	≈ 0	≈ 0	none
10	1.0000	1.0000	27,339	27,339	27,339
11	0.9995	1.0000	27,326	25,420	27,339
12	1.0000	0.0330	19,869	19,616	19,615
13	≈ 0	1.0000	≈ 0	≈ 0	none
14	≈ 0	1.0000	≈ 0	≈ 0	none
15	≈ 0	1.0000	≈ 0	≈ 0	none
16	≈ 0	1.0000	≈ 0	≈ 0	none
					$\sum = 187,816$

Table 2: Two-damper optimization of the eight-story asymmetric structure. All damping coefficients are in $\left[\frac{kN \cdot s}{m}\right]$.

5.3 Example 3: Eight-story three bay by three bay setback frame structure

In this example we consider another test case of an asymmetric reinforced concrete setback frame introduced by Tso and Yao [52]. Optimal design of added dampers was attained by [32] using uncorrelated continuous design variables for the damping coefficients. The structural properties are the same as for the full frame of example 2, but only one side of the structure rises to a height of eight stories, see Figure 5. Again, a single component of the ground motion in the "Y" direction is considered.

There are 16 potential damper locations (see Figure 5). All other parameters are identical

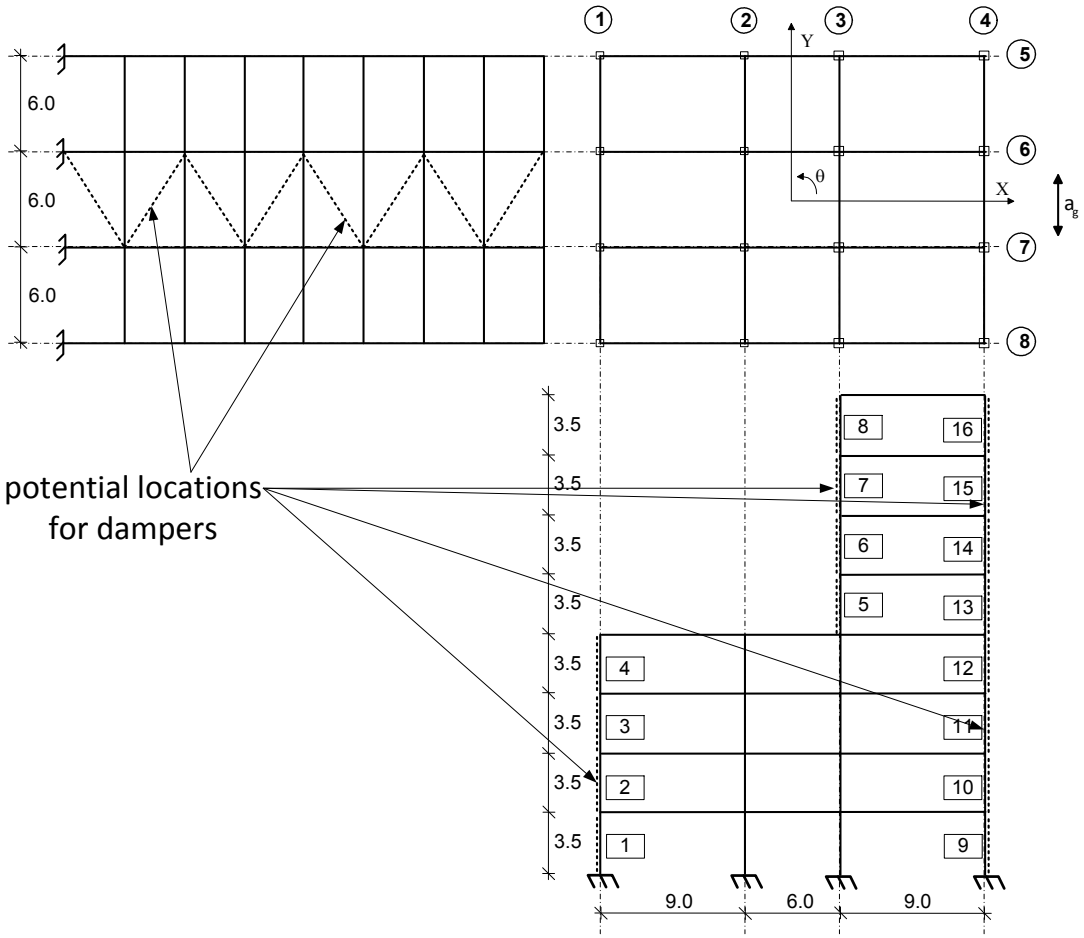

Figure 5: A setback 3D frame structure for example 3 [52].

to those used in Example 2. Optimization converged after 213 iterations, taking 50.1 seconds in MATLAB. A value of $y_1 = 0.3926$ was obtained, corresponding to an optimized damping coefficient of $19,629\left[\frac{kN\cdot s}{m}\right]$. The chosen locations of the dampers were in the second floor of frame 1 and in floors 2-4 in frame 4. The total added damping was therefore $78,515\left[\frac{kN\cdot s}{m}\right]$. With the resulting discrete design, the maximum violation of the constraint was 0.2% at location 10, corresponding to the second story in frame 4. No further constraint violations were encountered when evaluating with the complete ensemble.

Optimizing with two damper size groups, we maintained the same continuation scheme as for the full frame optimization in Example 2. Convergence was achieved after 246 iterations, taking 61.8 seconds in MATLAB. Values of $y_1 = 0.0373$ and $y_2 = 0.5000$ were obtained, corresponding to optimized damping coefficients of $1,866\left[\frac{kN\cdot s}{m}\right]$ and $25,000\left[\frac{kN\cdot s}{m}\right]$ respectively. The chosen locations of the dampers are presented in Table 3. It can be seen that the resulting design is in fact discrete and no interpretation is required. In principle, the feasible set of the problem with one damper size is a subset of the feasible set of the problem with two damper sizes. Therefore in an ideal setting where global optima can be reached, it is expected that the result with one size will not outperform the result with two sizes. This cannot be guaranteed in our approach which may converge to local minima due to the non-convexity of the problem. In this example, we in fact obtain an objective slightly inferior to that obtained with one damper size: 78,733 compared to 78,515. However, with two damper sizes the actual constraint violation is smaller: 0.04% at location 12, corresponding to the fourth story in frame 4. This implies that the design with two damper sizes indeed represents a better cost-performance trade-off than the design with one damper size. Concluding this example, the optimized design was evaluated with the other 19 ground motions in the ensemble and no other constraint violations were encountered

The setback frame example was used also for evaluating the increase in computational effort

Location	$\mathbf{x}_1$	$\mathbf{x}_2$	$\mathbf{c}_d$	$\widetilde{\mathbf{c}}_d$	Selected damper
1	≈ 0	0.8930	≈ 0	≈ 0	none
2	1.0000	1.0000	25,000	25,000	25,000
3	1.0000	≈ 0	1,866	1,866	1,866
4	≈ 0	0.8883	≈ 0	≈ 0	none
5	≈ 0	0.8973	≈ 0	≈ 0	none
6	≈ 0	0.5500	≈ 0	≈ 0	none
7	≈ 0	0.4628	≈ 0	≈ 0	none
8	≈ 0	0.3954	≈ 0	≈ 0	none
9	≈ 0	0.9150	≈ 0	≈ 0	none
10	1.0000	1.0000	25,000	25,000	25,000
11	1.0000	1.0000	25,000	25,000	25,000
12	1.0000	≈ 0	1,866	1,866	1,866
13	≈ 0	0.9011	≈ 0	≈ 0	none
14	≈ 0	0.1754	≈ 0	≈ 0	none
15	≈ 0	0.1610	≈ 0	≈ 0	none
16	≈ 0	0.2497	≈ 0	≈ 0	none
					$\sum = 78,733$

Table 3: Two-damper optimization of the eight-story setback structure. All damping coefficients are in $\left[\frac{kN \cdot s}{m}\right]$.

when the number of design variables increases. Considering all stories in frames 1-8 as potential locations results in 56 possible dampers. Therefore the number of "binary" design variables is 112, in addition to two continuous variables. Optimization with the first ground motion (LA16) required 271 iterations and took 79.8 seconds - only slightly longer than when 16 locations were considered. In the optimized design, two dampers with $25,000\left[\frac{kN \cdot s}{m}\right]$ were assigned to story 2 in frame 3 and to story 3 in frame 4. Four additional dampers with $6,478\left[\frac{kN \cdot s}{m}\right]$ were assigned to story 2 in frame 2, story 4 in frame 3, and stories 2 and 4 in frame 4. The final objective is therefore $75,912\left[\frac{kN \cdot s}{m}\right]$ - slightly lower than with 16 potential locations. From a strictly mathematical standpoint, this is sensible because in general enlarging the design space should result in better, or equivalent, solutions. However, from an engineer's perspective the proposed design stands in contrast to typical designs: The dampers are not placed in frame 1 which is one of the peripheral frames. This means that for the particular ground motion considered, the common choice of positioning dampers only in peripheral frames may not be the most economical. Evaluation of the optimized designs with respect to the complete ensemble reveals several drift violations. In principal, the problem should be solved while considering additional records. This is not presented in the paper. Moreover, this means that the design obtained with dampers strictly in the peripheral frames is most probably the best when considering all ground motions.

Focusing on the computational performance, it is clear that one of the big advantages of the proposed continuous-variable optimization scheme lies in its efficiency: The computational effort is not particularly sensitive to the number of design variables, as opposed to integer-variable optimization methods. Rather, it is proportional to the number of design iterations dictated by the continuation scheme, and to the costs of computations performed within each design cycle, consisting of: Structural analysis, sensitivity analysis and solution of the sub-problem.

6 Conclusions

In this paper a methodology for the optimal sizing and allocation of viscous dampers was presented. The methodology mimics the minimization of the sum, for all size groups of dampers, of the number of dampers of the given size group times the peak force expected in the most loaded damper of that size group. Constraints are assigned on peak envelope inter-story drifts of each story of each peripheral frame separately. These are computed based on a given ensemble of realistic ground motions. This results in a methodology that can be used for a practical performance-based design of retrofitting of 3D irregular frames.

The innovation of the proposed methodology lies in its formulation and corresponding optimization scheme that enable a more practical optimal design of dampers. In the proposed methodology continuous damping coefficients are optimally designed for the various size groups of dampers. These are assigned to the structure such that in each potential location for dampers a damper of a single size group, if any, is optimally allocated. This presents another step towards enabling an efficient use of optimization techniques in practice without having to interpret the attained designs.

The key for achieving an efficient optimization scheme for the challenging problem of damper placement and sizing lies in the adoption of material interpolation techniques, originally proposed in the context of continuum topology optimization. All discrete design variables that represent the existence of dampers are replaced by continuous variables, while intermediate values are implicitly penalized. As demonstrated in the examples, a similar computational effort was required for convergence even when the number of 0-1 design variables was increased from 16 (one damper size group, 16 locations) to 112 (two damper size groups, 56 locations). It is expected that the proposed methodology will facilitate efficient optimal design of dampers in large scale structures where the number of discrete design variables may be very large. This is also implied by the examples even though the number of design variables considered so far was significantly smaller than that expected to be handled effectively by the methodology.

References

[1] A. Agrawal and J. Yang. Optimal placement of passive dampers on seismic and wind-excited buildings using combinatorial optimization. *Journal of Intelligent Material Systems and Structures*, 10(12):997–1014, 1999.

[2] J. J. Aguirre, J. L. Almazán, and C. J. Paul. Optimal control of linear and nonlinear asymmetric structures by means of passive energy dampers. *Earthquake engineering & structural dynamics*, 42(3):377–395, 2013.

[3] J. L. Almazán and J. C. de la Llera. Torsional balance as new design criterion for asymmetric structures with energy dissipation devices. *Earthquake Engineering & Structural Dynamics*, 38(12):1421–1440, 2009.

[4] T. Attard. Controlling all interstory displacements in highly nonlinear steel buildings using optimal viscous damping. *Journal of Structural Engineering*, 133(9):1331–1340, 2007.

[5] E. Aydin, M. Boduroglu, and D. Guney. Optimal damper distribution for seismic rehabilitation of planar building structures. *Engineering Structures*, 29(2):176–185, 2007.

[6] M. P. Bendsøe. Optimal shape design as a material distribution problem. *Structural Optimization*, 1:193–202, 1989.

[7] M. P. Bendsøe and N. Kikuchi. Generating optimal topologies in structural design using a homogenization method. *Computer Methods in Applied Mechanics and Engineering*, 71: 197–224, 1988.

[8] M. P. Bendsøe and O. Sigmund. Material interpolation schemes in topology optimization. *Archive of Applied Mechanics*, 69(9-10):635–654, 1999.

[9] M. P. Bendsøe and O. Sigmund. *Topology Optimization - Theory, Methods and Applications*. Springer, Berlin, 2003.

[10] V. V. Bertero. Performance-based seismic engineering: A critical review of proposed guidelines. *Seismic design methodologies for the next generation of codes*, pages 1–31, 1997.

[11] E. W. Cheney and A. A. Goldstein. Newton's method for convex programming and Tchebycheff approximation. *Numerische Mathematik*, 1(1):253–268, 1959.

[12] A. K. Chopra. *Dynamics of structures: Theory and applications to earthquake engineering*, volume 2. Prentice Hall Saddle River NY, 2001.

[13] C. Christopoulos and A. Filiatrault. *Principles of passive supplemental damping and seismic isolation*. IUSS Press, 2006.

[14] M. C. Constantinou and M. Symans. *Experimental and analytical investigation of seismic response of structures with supplemental fluid viscous dampers*. National Center for earthquake engineering research, 1992.

[15] G. Dargush and R. Sant. Evolutionary aseismic design and retrofit of structures with passive energy dissipation. *Earthquake engineering & structural dynamics*, 34(13):1601–1626, 2005.

[16] FEMA. *Prestandard and Commentary for the Seismic Rehabilitation of Buildings*. Federal Emergency Management Agency, 2000.

[17] M. García, J. C. de la Llera, and J. L. Almazán. Torsional balance of plan asymmetric structures with viscoelastic dampers. *Engineering Structures*, 29(6):914–932, 2007.

[18] N. Gluck, A. Reinhorn, J. Gluck, and R. Levy. Design of supplemental dampers for control of structures. *Journal of structural Engineering*, 122(12):1394–1399, 1996.

[19] R. K. Goel. Effects of supplemental viscous damping on seismic response of asymmetric-plan systems. *Earthquake engineering & structural dynamics*, 27(2):125–141, 1998.

[20] R. K. Goel. Seismic behaviour of asymmetric buildings with supplemental damping. *Earthquake engineering & structural dynamics*, 29(4):461–480, 2000.

[21] G. Hahn and K. Sathiavageeswaran. Effects of added-damper distribution on the seismic response of buildings. *Computers & structures*, 43(5):941–950, 1992.

[22] C. F. Hvejsel and E. Lund. Material interpolation schemes for unified topology and multi-material optimization. *Structural and Multidisciplinary Optimization*, 43(6):811–825, 2011.

[23] J.-S. Hwang, Y.-N. Huang, S.-L. Yi, and S.-Y. Ho. Design formulations for supplemental viscous dampers to building structures. *Journal of structural engineering*, 134(1):22–31, 2008.

[24] Y. Kanno. Damper placement optimization in a shear building model with discrete design variables: a mixed-integer second-order cone programming approach. *Earthquake Engineering & Structural Dynamics*, pages n/a–n/a, 2013. doi: 10.1002/eqe.2292.

[25] J. E. Kelley, Jr. The cutting-plane method for solving convex programs. *Journal of the Society for Industrial & Applied Mathematics*, 8(4):703–712, 1960.

[26] J. Kim and S. Bang. Optimum distribution of added viscoelastic dampers for mitigation of torsional responses of plan-wise asymmetric structures. *Engineering structures*, 24(10): 1257–1269, 2002.

[27] O. Lavan. On the efficiency of viscous dampers in reducing various seismic responses of wall structures. *Earthquake Engineering & Structural Dynamics*, 41(12):1673–1692, 2012.

[28] O. Lavan and M. Avishur. Seismic behavior of viscously damped yielding frames under structural and damping uncertainties. *Bulletin of Earthquake Engineering*, pages 1–24, 2013.

[29] O. Lavan and G. F. Dargush. Multi-objective evolutionary seismic design with passive energy dissipation systems. *Journal of Earthquake Engineering*, 13(6):758–790, 2009.

[30] O. Lavan and R. Levy. Optimal design of supplemental viscous dampers for irregular shear-frames in the presence of yielding. *Earthquake engineering & structural dynamics*, 34(8): 889–907, 2005.

[31] O. Lavan and R. Levy. Optimal design of supplemental viscous dampers for linear framed structures. *Earthquake engineering & structural dynamics*, 35(3):337–356, 2006.

[32] O. Lavan and R. Levy. Optimal peripheral drift control of 3d irregular framed structures using supplemental viscous dampers. *Journal of Earthquake Engineering*, 10(06):903–923, 2006.

[33] R. Levy and O. Lavan. Fully stressed design of passive controllers in framed structures for seismic loadings. *Structural and Multidisciplinary Optimization*, 32(6):485–498, 2006.

[34] R. Levy and O. Lavan. Quantitative comparison of optimization approaches for the design of supplemental damping in earthquake engineering practice. *Journal of structural engineering*, 135(3):321–325, 2009.

[35] W.-H. Lin and A. K. Chopra. Understanding and predicting effects of supplemental viscous damping on seismic response of asymmetric one-storey systems. *Earthquake engineering & structural dynamics*, 30(10):1475–1494, 2001.

[36] W.-H. Lin and A. K. Chopra. Asymmetric one-storey elastic systems with non-linear viscous and viscoelastic dampers: Earthquake response. *Earthquake engineering & structural dynamics*, 32(4):555–577, 2003.

[37] W.-H. Lin and A. K. Chopra. Asymmetric one-storey elastic systems with non-linear viscous and viscoelastic dampers: Simplified analysis and supplemental damping system design. *Earthquake engineering & structural dynamics*, 32(4):579–596, 2003.

[38] D. Lopez Garcia and T. Soong. Efficiency of a simple approach to damper allocation in mdof structures. *Journal of Structural Control*, 9(1):19–30, 2002.

[39] M. Palermo, S. Muscio, S. Silvestri, L. Landi, and T. Trombetti. On the dimensioning of viscous dampers for the mitigation of the earthquake-induced effects in moment-resisting frame structures. *Bulletin of Earthquake Engineering*, pages 1–18, 2013.

[40] Y.-J. Park and A. H.-S. Ang. Mechanistic seismic damage model for reinforced concrete. *Journal of Structural Engineering*, 111(4):722–739, 1985.

[41] M. Priestley. Performance based seismic design. *Bulletin of the New Zealand Society for Earthquake Engineering*, 33(3):325–346, 2000.

[42] O. Sigmund and M. P. Bendsøe. Topology optimization: from airplanes to nano-optics. In K. Stubkjær and T. Kortenbach, editors, *Bridging from Technology to Society*. Technical University of Denmark, Lyngby, Denmark, 2004.

[43] M. P. Singh and L. M. Moreschi. Optimal seismic response control with dampers. *Earthquake engineering & structural dynamics*, 30(4):553–572, 2001.

[44] P. G. Somerville and S. J. Venture. *Development of ground motion time histories for phase 2 of the FEMA/SAC steel project*. SAC Joint Venture, 1997.

[45] T. T. Soong and G. F. Dargush. *Passive energy dissipation systems in structural engineering*. Wiley New York, 1997.

[46] J. Stegmann and E. Lund. Discrete material optimization of general composite shell structures. *International Journal for Numerical Methods in Engineering*, 62(14):2009–2027, 2005.

[47] M. Stolpe and K. Svanberg. An alternative interpolation scheme for minimum compliance topology optimization. *Structural and Multidisciplinary Optimization*, 22(2):116–124, 2001.

[48] M. Symans and M. Constantinou. Passive fluid viscous damping systems for seismic energy dissipation. *ISET Journal of Earthquake Technology*, 35(4):185–206, 1998.

[49] I. Takewaki. Optimal damper placement for minimum transfer functions. *Earthquake engineering & structural dynamics*, 26(11):1113–1124, 1997.

[50] I. Takewaki. *Building control with passive dampers: optimal performance-based design for earthquakes*. Wiley, 2011.

[51] I. Takewaki, S. Yoshitomi, K. Uetani, and M. Tsuji. Non-monotonic optimal damper placement via steepest direction search. *Earthquake engineering & structural dynamics*, 28(6):655–670, 1999.

[52] W. Tso and S. Yao. Seismic load distribution in buildings with eccentric setback. *Canadian Journal of Civil Engineering*, 21(1):50–62, 1994.

[53] J. Whittle, M. Williams, T. L. Karavasilis, and A. Blakeborough. A comparison of viscous damper placement methods for improving seismic building design. *Journal of Earthquake Engineering*, 16(4):540–560, 2012.

[54] B. Wu, J.-P. Ou, and T. Soong. Optimal placement of energy dissipation devices for three-dimensional structures. *Engineering Structures*, 19(2):113–125, 1997.

[55] J. Yang, S. Lin, J.-H. Kim, and A. Agrawal. Optimal design of passive energy dissipation systems based on h? and h2 performances. *Earthquake engineering & structural dynamics*, 31 (4):921–936, 2002.

[56] R.-H. Zhang and T. Soong. Seismic design of viscoelastic dampers for structural applications. *Journal of Structural Engineering*, 118(5):1375–1392, 1992.